

Polarization-independent two-dimensional beam steering using liquid crystal optical phased arrays

Liang Wu (吴亮)^{1,2}, Xiangru Wang (汪相如)^{2,*}, Caidong Xiong (熊彩东)¹,
Ziqiang Huang (黄子强)³, Rusheng Zhuo (卓儒盛)², Jiarui Rao (饶家睿)²,
and Qinggui Tan (谭庆贵)⁴

¹*School of Physical Electronics, University of Electronic Science and Technology of China, Chengdu 610054, China*

²*School of Optoelectronic Information, University of Electronic Science and Technology of China, Chengdu 610054, China*

³*Research Institute of Electronic Science and Technology, University of Electronic Science and Technology of China, Chengdu 610054, China*

⁴*National Key Laboratory of Science and Technology on Space Microwave, Xi'an 710100, China*

*Corresponding author: xiangruwang@uestc.edu.cn

Received May 17, 2017; accepted July 14, 2017; posted online August 9, 2017

A polarization-independent nonmechanical laser beam steering scheme is proposed to realize continuous two-dimensional (2D) scanning with high efficiency, where the core components are two polarization-dependent devices, which are called liquid crystal optical phased arrays (LC-OPAs). These two one-dimensional (1D) devices are orthogonally cascaded to work on the state of azimuthal and elevation steering, respectively. Properties of polarization independence as well as 2D beam steering are mathematically and experimentally verified with a good agreement. Based on the experimental setup, linearly polarized beams with different polarization angles are steered with high accuracy. The measured angular deviations are less than 5 μrad , which is on the same order of the accuracy of the measurement system. This polarization-independent 2D laser beam steering scheme has potential application for nonmechanical laser communication, lidar, and other LC-based systems.

OCIS codes: 160.3710, 120.4820, 230.3720, 230.6120.

doi: 10.3788/COL201715.101601.

Nonmechanical laser beam steering has a great attraction in numerous laser applications, such as free-space optical (FSO) communication and lidar^[1,2]. Multiple alternative approaches to accomplish nonmechanical beam steering have been investigated, including micro-electromechanical mirrors (MEMs)^[3], lead lanthanum zirconate titanate (PLZT)^[4], microlens arrays^[5], and liquid crystal (LC)^[6-8]. Meanwhile, an LC-based optical phased array (LC-OPA) is one of the most promising candidates to be a nonmechanical beam steerer, owing to its advantages of low driving voltage, real-time programmable, mega pixels, low cost, and so on^[9-11]. It is an array of phase shifters, where the working medium of phase modulation is LC. A laser beam can be steered when an electric field is imposed on the individually addressable electrodes^[12,13]. The slow response time is one of the shortcomings for commercial LC-OPA devices using the material of E7 or similar nematic LC, and a couple of approaches have been investigated to improve the response time, including dual-frequency LC (DFLC), ferroelectric LC (FLC), and blue phase LC (BPLC), and so on. Meanwhile, due to the intrinsic optical anisotropy of LCs, the most commonly used LC-OPAs are strongly dependent on the polarization state of incident light^[14]. To develop polarization-independent LC devices, several methods have been proposed. One of the most promising methods is polymer-stabilized BPLC (PS-BPLC), as reported by Peng *et al.* for spatial light modulators and by Li *et al.* for adaptive lenses^[15,16]. But, these

methods have some problems, such as complicated fabrication process, insufficient phase change, or high operation voltage. From a device aspect, the application of conventional nematic LC-OPA is still very extensive nowadays, because of the low driving voltage and deep phase modulation. From a practical application aspect, i.e., FSO communication, the LC-OPA is not only used as a transmitter to deflect laser beams, but also as a receiver to steer the arriving laser beam into the local terminal. Because the attitude of satellite is always changing, it is almost impossible to know the polarization state of the incident arriving beam or hard to rapidly adjust the position of the LC-OPA in real-time^[17,18]. Therefore, it is considerably beneficial to develop a polarization-independent nonmechanical laser beam steering scheme for commercial LC-OPAs.

In this Letter, a novel optical setup based on two high-spatial-resolution LC-OPAs is proposed for polarization-independent two-dimensional (2D) beam steering^[19]. As illustrated in Fig. 1, the setup comprises a polarization beam splitter (PBS), a half-wave plate (HWP), two mirrors, and two LC-OPAs. Wherein, the two LC-OPAs are 1D, transmissive, and polarization-dependent devices, which can steer the laser beam in azimuthal or elevation angles. From Fig. 1, the incoming unpolarized beam is split into two linearly polarized beams (x polarization and y polarization) by the PBS. The fast axis of the HWP is oriented at 45° to the x axis, which enables polarization exchange between the x polarization and

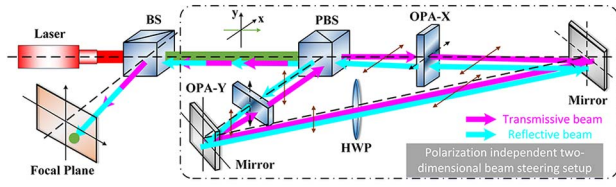


Fig. 1. (Color online) Schematic diagram of the polarization-independent 2D beam steering setup, where the 1D LC-OPAs are used.

y polarization. To make sure of full phase modulation of LC-OPAs, the optical axes of OPA-X and OPA-Y are arranged to be parallel to the polarization direction of the transmissive (x -polarization) and reflective (y -polarization) beams, respectively. As a result, the light path, which connects the PBS, OPA-X, mirror, and HWP is x polarized, and the light path that links the PBS, OPA-Y, mirror, and HWP is y polarized.

The mechanism of polarization-independent 2D beam steering of the scheme can be proven as follows. Assuming that the electric field of the normal incident beam can be expressed as

$$\mathbf{E}_{\text{in}} = A_x \cdot e^{i\delta_x} \cdot \mathbf{x} + A_y \cdot e^{i\delta_y} \cdot \mathbf{y}, \quad (1)$$

where δ_x and δ_y are the initial phase terms of the two components, A_x and A_y are the initial amplitudes, and \mathbf{x} and \mathbf{y} are unit vectors along the x and y axes, respectively. For the transmissive beam (x polarization) propagating clockwise (magenta color arrows), it is first modulated by OPA-X with phase modulation Φ_X . This steered beam is reflected by the mirror and then rotated 90° to be y polarization after passing through the HWP. It will be reflected again by another mirror and modulated by OPA-Y with phase modulation Φ_Y . Thus, the electric field of the outgoing beam on OPA-Y should be

$$\mathbf{E}_{\text{trans}} = e^{-i\phi_Y} \cdot [e^{-i\phi_X} \cdot (A_x \cdot e^{i\delta_x})] \cdot \mathbf{y}. \quad (2)$$

Similarly, the reflective beam (y polarization) propagating counterclockwise (cyan color arrows) is first modulated by OPA-Y with phase modulation Φ_Y and is modulated by OPA-X with phase modulation Φ_X . So, the electric field of the outgoing beam on OPA-X should be

$$\mathbf{E}_{\text{reflec}} = e^{-i\phi_X} \cdot [e^{-i\phi_Y} \cdot (A_y \cdot e^{i\delta_y})] \cdot \mathbf{x}. \quad (3)$$

Finally, the two modulated beams will be recombined again on the PBS to be an unpolarized output beam \mathbf{E}_{out} . The electric field of the outgoing beam becomes

$$\mathbf{E}_{\text{out}} = e^{-i\phi_X} \cdot e^{-i\phi_Y} \cdot [(A_y \cdot e^{i\delta_y}) \cdot \mathbf{x} + (A_x \cdot e^{i\delta_x}) \cdot \mathbf{y}]. \quad (4)$$

Comparing Eqs. (1) and (4), the amplitude and phase of x and y components of the incident beam are both still

involved in the output beam \mathbf{E}_{out} . But, the polarization state is rotated with 90° , in other words, the x and y components are exchanged with each other. Hence, the setup is polarization independent.

Moreover, owing to the bidirectional loop structure, both x and y components of the incident beam experience a same phase modulation by the two LC-OPAs. The total phase modulation of $e^{-i\phi_X} \cdot e^{-i\phi_Y}$ indicates that a 2D beam steering can be obtained on the far-field after a relatively long distance propagation. When the LC-OPAs are driven on the method of variable period grating^[5], the phase modulation Φ_X and Φ_Y will be realized when we apply the deflection data on each LC-OPA.

The property of polarization-independent 2D beam steering is verified by the experimental setup, as shown in Fig. 2(a). The collimated laser beam (red color) with a wavelength of $\lambda = 1064 \text{ nm}$ is adjusted by the first PBS and HWP, so that a variable linearly polarized light (green color) can be produced. For convenience, a beam splitter (BS) is used to deliver the polarized beam into the setup and reflect the steered beam from the loop to the far-field. The BS would result in optical loss for the whole system when the beam passes through the BS twice, so a polarization-independent BS device should be adopted in practical system design, such as a polarization-independent optical circulator. When the linearly polarized beam is incident on the second PBS, two polarized beams are generated in the loop, one is a transmissive beam with x polarization (cyan color), and another is a reflective beam with y polarization (magenta color). A Fourier lens with a focal length of $f = 42 \text{ cm}$ is settled on the far-field. A beam profiler (Ophir-Spiricon, SP620U) is placed on the focus of the lens to measure the diffraction patterns and the steering angles.

The two 1D LC-OPA devices are fabricated, and the associated parameters are as follows: the number of array electrodes is 1920, the pixel pitch is $5 \mu\text{m}$, so that the effective optical aperture is $10 \text{ mm} \times 15 \text{ mm}$. The thickness of the LC layer is $9 \mu\text{m}$, and the nematic LC of E7-F (homemade, $\Delta n = 0.15$) is filled in the LC cells as the medium of phase modulation. Meanwhile, in the planar LC cell, the top and bottom substrate are rubbed in antiparallel with a pre-tilt angle of 2° , and polyimide (ZKPI-410) is used as the alignment layers to impose anchoring for the LC. The voltage-dependent phase

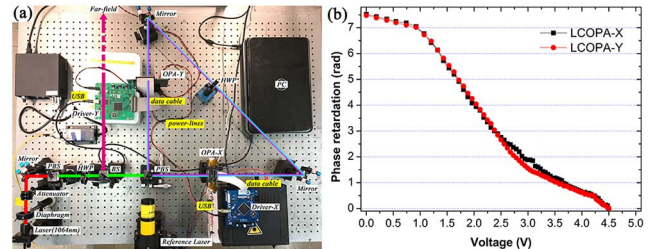


Fig. 2. (Color online) (a) Experimental setup of the polarization-independent 2D beam steering. (b) Measured phase retardation versus driving voltage.

retardation of the two LC-OPAs is experimentally obtained at 1064 nm, as shown in Fig. 2(b). The curves show that the threshold voltage is about 1 V, and the maximum driving voltage is 4.5 V. The device of LC-OPA is driven by four integrated circuit (IC) chips, which connect to the driver electronics with a data cable. The drivers are used to load data to each LC-OPA, and the deflection data are generated by a personal computer (PC), according to the method of variable period grating. Note that the crystal axis of LC-OPAs are parallel to the polarization direction of the corresponding beams, which output from the second PBS. The success of the experiment depends on the factor that is the calibration of light path, especially since the transmissive beam and reflective beam in the loop should be completely coaxial and parallel to the optical platform, so that the two beams will be recombined on the PBS. For simplicity, the loop is arranged to be an isosceles right-angled triangle. Meanwhile, a reference laser ($\lambda = 632.8$ nm) is used to calibrate the light path during the calibration procedure. All of the experiments were carried out at room temperature.

As an example of three desired 2D steering angles, the measured output steering angles in the x (azimuth) and y (elevation) direction versus different polarization angles of the linearly polarized beam are depicted in Fig. 3. The polarization angle is the included angle between the polarization direction of the incident beam and the x direction. The output steering angles are calculated by the centroid algorithm $\theta_{\text{out}} = (x - x_0)/f$, where x and x_0 are the measured locations of the output steering beam and initial beam, respectively, and f is the focal length of the Fourier lens. Meanwhile, the original location is marked by a red circle and remains unchanged for all cases. The centroid location is captured by the crosshair, which can track the position of the output beam automatically.

As shown in Fig. 3, the incident beams are steered to the angles as we desired, and the measured steering angles under different polarizations are plotted in Fig. 3. All of

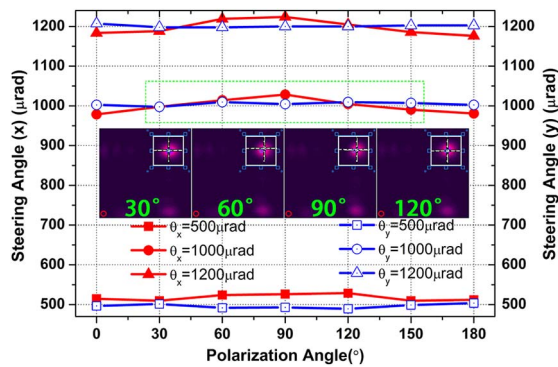


Fig. 3. (Color online) Measured output steering angles in x (azimuth) and y (elevation) direction versus different polarization angles of the linearly polarized beam. Inserted figures are the captured beam patterns of several polarization states under the steering angle of $(\theta_x, \theta_y) = (1000, 1000)$ μrad .

the curves are approximately linear, indicating that the locations of the steering beams remain basically invariable as the polarization angle changes. Particularly, the angular errors are less than 5 μrad in the y direction, which demonstrates a high accuracy of beam steering in the y direction. However, larger angular deviations appear in the x direction, whose maximum value is about 25 μrad , and it is about five times larger than that in the y direction. The different angular deviation between the x and y direction results from the optical path error of the system. When we calibrated the light path to keep the two beams to be coaxial in the loop, it is easier to ensure their altitude (y direction), i.e., by using two diaphragms, but harder to completely ensure their overlap in the x direction. Thus, the imperfect alignment of the x and y polarized beam is the cause of additional steering errors. In addition, the error of the experimental phase modulation curve of the device and the PBS would give rise to the angular deviation.

Furthermore, the captured beam patterns of several polarization states under the steering angle of $(\theta_x, \theta_y) = (1000, 1000)$ μrad are inserted in Fig. 3. Meanwhile, the white square box is a manual aperture to positioning the steering beams. Compared with these figures, it is clear that the locations and intensity of the steering beams are almost the same whatever the polarization state of the incident beam are. Therefore, these experimental results demonstrate a good agreement with the expected results, as we designed. Meanwhile, some other unsharp beam spots that are called grating lobes, also appear in the far-field. Such grating lobes will result in efficiency loss because of the periodicity of phase modulation and the fringing effect of LC-OPAs. Moreover, the diffraction efficiency of the LC-OPA is listed in Table 1, the values before and after optimization are experimentally measured and demonstrated by Xiao *et al.*^[20]. Thus, a further optimization process for the LC-OPA and calibration for the setup are required so that we can use them in practical systems.

To characterize the polarization properties of the setup, a polarizer is placed in front of the beam profiler to measure the polarization components. Figure 4 shows the beam patterns of output beams and corresponding polarization components at three polarization angles when the desired steering angle is (700, 800) μrad . From Figs. 4(a) to 4(c), the polarization angles of the linearly polarized incident beam are 0°, 45°, and 90°, respectively. The first column is the overall output beams without using a polarizer, the second and third columns are the x -polarized and y -polarized components detected by a polarizer, respectively.

Table 1. Diffraction Efficiency of the LC-OPA

	3.050°	1.524°	0.762°	0.381°	0.190°
Before optimization	20.6%	38.2%	47.7%	50.2%	56.4%
After optimization	65.2%	72.0%	78.6%	81.8%	84.7%

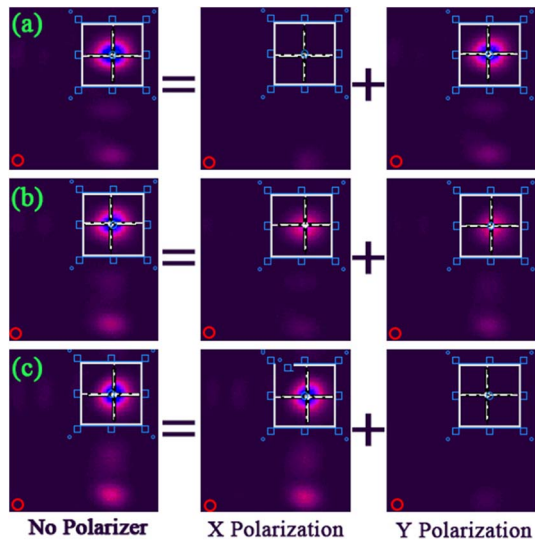


Fig. 4. Beam patterns of output beams and corresponding polarization components at three different polarization angles. Polarization angles of the linearly polarized incident beam are: (a) 0° , (b) 45° , and (c) 90° . The steering angle is $(700, 800) \mu\text{rad}$.

As shown in Fig. 4, when the incident beam is x polarized, the x component is zero, while the y component is almost the same as the overall output beam. Vice versa, for the y -polarized incident beam, the y component is zero, while the x component is almost the same as the overall output beam. For the 45° -polarization incident beam, the x and y components are almost equal, and the intensity of the two components is half of the overall output beam. These results show that the output steering beam contains the amplitude and phase information of both orthogonal (x - and y -polarization) components of the incident beam. The two polarized components are modulated effectively by the two LC-OPAs, resulting in an excellent light efficiency of the setup. The figures also indicate that the polarization state of the output steering beam is rotated with 90° with respect to the incident beam. It is because the polarization direction of the x and y components is exchanged after passing through the HWP. From the application point of view, if the polarization state should be taken into account, i.e., the communication system, an HWP may be added in the system to rotate the polarization state back.

In conclusion, we establish and demonstrate a novel setup for polarization-independent 2D laser beam steering by adopting two polarization-dependent 1D LC-OPAs. This simple but smart scheme can successfully modulate an unpolarized incident laser beam in two dimensions with high steering accuracy. The polarization characteristics of the setup are measured by extracting the polarization components of the output steering beam. All of the theoretical analysis and experimental evidence are presented to verify the mechanism of the polarization-independent 2D beam steering setup. This polarization-independent scheme enables the LC-OPAs to be highly promising for the nonmechanical laser communication, lidar, and other LC-based applications.

This work was supported by the National Science Foundation of China (NSFC) (Nos. 61405029, 91438108, and 61231012) and the Shanghai Aerospace Science and Technology (SAST) (No. 2015087).

References

1. A. K. Majumdar and J. C. Ricklin, *Free-space Laser Communications: Principles and Advances* (Springer, 2010), Vol. 2.
2. P. F. McManamon, *Liq. Cryst.: Opt. Appl.* **5947**, 59470I (2005).
3. B. W. Yoo, M. Megens, T. Sun, and W. Yang, *Opt. Express* **22**, 19029 (2014).
4. G. Hu, Z. Qi, B. Yun, R. Zhang, and Y. Cui, *Chin. Opt. Lett.* **13**, 111301 (2015).
5. F. Zhao, M. Zhu, and P. Zhan, *Chin. Opt. Lett.* **8**, 508 (2010).
6. P. F. McManamon, *Opt. Eng.* **32**, 2657 (1993).
7. D. P. Resler, D. S. Hobbs, R. C. Sharp, L. J. Friedman, and T. A. Dorschner, *Opt. Lett.* **21**, 689 (1996).
8. B. Zhang, S. Liu, X. Tang, and J. Lu, *Chin. Opt. Lett.* **14**, 090604 (2016).
9. P. F. McManamon and P. J. Bos, *Proc. IEEE* **97**, 1078 (2009).
10. J. Stockley and S. Steven, *Proc. SPIE* **5550**, 32 (2004).
11. Z. Zhang, Z. You, and D. Chu, *Light: Sci. Appl.* **3**, e213 (2014).
12. R. G. Lindquist, T. M. Leslie, and J. H. Kulick, *Opt. Lett.* **19**, 670 (1994).
13. P. F. McManamon and T. A. Dorschner, *Proc. IEEE* **84**, 268 (1996).
14. S. R. Harris, *Proc. SPIE* **5213**, 26 (2003).
15. F. Peng, Y. H. Lee, Z. Luo, and S. T. Wu, *Opt. Lett.* **40**, 5097 (2015).
16. Y. Li and S. T. Wu, *Opt. Express* **19**, 8045 (2011).
17. B. Winker and M. Mahajan, in *Proceedings of IEEE Aerospace Conference* (2004), p. 1702.
18. L. Wu, X. Wang, and C. Xiong, *Opt. Eng.* **55**, 116115 (2016).
19. S. T. Wu and C. S. Wu, *Jpn. J. Appl. Phys.* **35**, 5349 (1996).
20. F. Xiao, L. Kong, and J. Chen, *Appl. Opt.* **56**, 4585 (2017).